FERMILAB-PUB-XX-YYY-Z CDF/PHYS/ELECTROWEAK/PUBLIC/10311

Search for $WZ + ZZ$ production with $\not\!\!E_T$ + jets with b enhancement at $\sqrt{s} = 1.96$ TeV

T. Aaltonen,[21] B. Álvarez González[w],[9] S. Amerio,[41] D. Amidei,[32] A. Anastassov,[36] A. Annovi,[17] J. Antos,[12] G. Apollinari,[15] J.A. Appel,[15] A. Apresyan,[46] T. Arisawa,[56] A. Artikov,[13] J. Asaadi,[51] W. Ashmanskas,[15] B. Auerbach,[59] A. Aurisano,[51] F. Azfar,[40] W. Badgett,[15] A. Barbaro-Galtieri,[26] V.E. Barnes,[46] B.A. Barnett,[23] P. Barria[dd],[44] P. Bartos,[12] M. Bauce[bb],[41] G. Bauer,[30] F. Bedeschi,[44] D. Beecher,[28] S. Behari,[23] G. Bellettini[cc],[44] J. Bellinger,[58] D. Benjamin,[14] A. Beretvas,[15] A. Bhatti,[48] M. Binkley*,[15] D. Bisello[bb],[41] I. Bizjak[hh],[28] K.R. Bland,[5] B. Blumenfeld,[23] A. Bocci,[14] A. Bodek,[47] D. Bortoletto,[46] J. Boudreau,[45] A. Boveia,[11] L. Brigliadori[aa],[6] A. Brisuda,[12] C. Bromberg,[33] E. Brucken,[21] M. Bucciantonio[cc],[44] J. Budagov,[13] H.S. Budd,[47] S. Budd,[22] K. Burkett,[15] G. Busetto[bb],[41] P. Bussey,[19] A. Buzatu,[31] C. Calancha,[29] S. Camarda,[4] M. Campanelli,[28] M. Campbell,[32] F. Canelli[11],[15] B. Carls,[22] D. Carlsmith,[58] R. Carosi,[44] S. Carrillo[k],[16] S. Carron,[15] B. Casal,[9] M. Casarsa,[15] A. Castro[aa],[6] P. Catastini,[20] D. Cauz,[52] V. Cavaliere,[22] M. Cavalli-Sforza,[4] A. Cerri[e],[26] L. Cerrito[q],[28] Y.C. Chen,[1] M. Chertok,[7] G. Chiarelli,[44] G. Chlachidze,[15] F. Chlebana,[15] K. Cho,[25] D. Chokheli,[13] J.P. Chou,[20] W.H. Chung,[58] Y.S. Chung,[47] C.I. Ciobanu,[42] M.A. Ciocci[dd],[44] A. Clark,[18] C. Clarke,[57] G. Compostella[bb],[41] M.E. Convery,[15] J. Conway,[7] M.Corbo,[42] M. Cordelli,[17] C.A. Cox,[7] D.J. Cox,[7] F. Crescioli[cc],[44] C. Cuenca Almenar,[59] J. Cuevas[w],[9] R. Culbertson,[15] D. Dagenhart,[15] N. d'Ascenzo[u],[42] M. Datta,[15] P. de Barbaro,[47] S. De Cecco,[49] G. De Lorenzo,[4] M. Dell'Orso[cc],[44] C. Deluca,[4] L. Demortier,[48] J. Deng[b],[14] M. Deninno,[6] F. Devoto,[21] M. d'Errico[bb],[41] A. Di Canto[cc],[44] B. Di Ruzza,[44] J.R. Dittmann,[5] M. D'Onofrio,[27] S. Donati[cc],[44] P. Dong,[15] M. Dorigo,[52] T. Dorigo,[41] K. Ebina,[56] A. Elagin,[51] A. Eppig,[32] R. Erbacher,[7] D. Errede,[22] S. Errede,[22] N. Ershaidat[z],[42] R. Eusebi,[51] H.C. Fang,[26] S. Farrington,[40] M. Feindt,[24] J.P. Fernandez,[29] C. Ferrazza[ee],[44] R. Field,[16] G. Flanagan[s],[46] R. Forrest,[7] M.J. Frank,[5] M. Franklin,[20] J.C. Freeman,[15] Y. Funakoshi,[56] I. Furic,[16] M. Gallinaro,[48] J. Galyardt,[10] J.E. Garcia,[18] A.F. Garfinkel,[46] P. Garosi[dd],[44] H. Gerberich,[22] E. Gerchtein,[15] S. Giagu[ff],[49] V. Giakoumopoulou,[3] P. Giannetti,[44] K. Gibson,[45] C.M. Ginsburg,[15] N. Giokaris,[3] P. Giromini,[17] M. Giunta,[44] G. Giurgiu,[23] V. Glagolev,[13] D. Glenzinski,[15] M. Gold,[35] D. Goldin,[51] N. Goldschmidt,[16] A. Golossanov,[15] G. Gomez,[9] G. Gomez-Ceballos,[30] M. Goncharov,[30] O. González,[29] I. Gorelov,[35] A.T. Goshaw,[14] K. Goulianos,[48] S. Grinstein,[4] C. Grosso-Pilcher,[11] R.C. Group[55],[15] J. Guimaraes da Costa,[20] Z. Gunay-Unalan,[33] C. Haber,[26] S.R. Hahn,[15] E. Halkiadakis,[50] A. Hamaguchi,[39] J.Y. Han,[47] F. Happacher,[17] K. Hara,[53] D. Hare,[50] M. Hare,[54] R.F. Harr,[57] K. Hatakeyama,[5] C. Hays,[40] M. Heck,[24] J. Heinrich,[43] M. Herndon,[58] S. Hewamanage,[5] D. Hidas,[50] A. Hocker,[15] W. Hopkins[f],[15] D. Horn,[24] S. Hou,[1] R.E. Hughes,[37] M. Hurwitz,[11] U. Husemann,[59] N. Hussain,[31] M. Hussein,[33] J. Huston,[33] G. Introzzi,[44] M. Iori[ff],[49] A. Ivanov[o],[7] E. James,[15] D. Jang,[10] B. Jayatilaka,[14] E.J. Jeon,[25] M.K. Jha,[6] S. Jindariani,[15] W. Johnson,[7] M. Jones,[46] K.K. Joo,[25] S.Y. Jun,[10] T.R. Junk,[15] T. Kamon,[51] P.E. Karchin,[57] A. Kasmi,[5] Y. Kato[n],[39] W. Ketchum,[11] J. Keung,[43] V. Khotilovich,[51] B. Kilminster,[15] D.H. Kim,[25] H.S. Kim,[25] H.W. Kim,[25] J.E. Kim,[25] M.J. Kim,[17] S.B. Kim,[25] S.H. Kim,[53] Y.K. Kim,[11] N. Kimura,[56] M. Kirby,[15] S. Klimenko,[16] K. Kondo*,[56] D.J. Kong,[25] J. Konigsberg,[16] A.V. Kotwal,[14] M. Kreps,[24] J. Kroll,[43] D. Krop,[11] N. Krumnack[l],[5] M. Kruse,[14] V. Krutelyov[c],[51] T. Kuhr,[24] M. Kurata,[53] S. Kwang,[11] A.T. Laasanen,[46] S. Lami,[44] S. Lammel,[15] M. Lancaster,[28] R.L. Lander,[7] K. Lannon[v],[37] A. Lath,[50] G. Latino[cc],[44] T. LeCompte,[2] E. Lee,[51] H.S. Lee,[11] J.S. Lee,[25] S.W. Lee[x],[51] S. Leo[cc],[44] S. Leone,[44] J.D. Lewis,[15] A. Limosani[r],[14] C.-J. Lin,[26] J. Linacre,[40] M. Lindgren,[15] E. Lipeles,[43] A. Lister,[18] D.O. Litvintsev,[15] C. Liu,[45] Q. Liu,[46] T. Liu,[15] S. Lockwitz,[59] A. Loginov,[59] D. Lucchesi[bb],[41] J. Lueck,[24] P. Lujan,[26] P. Lukens,[15] G. Lungu,[48] J. Lys,[26] R. Lysak,[12] R. Madrak,[15] K. Maeshima,[15] K. Makhoul,[30] S. Malik,[48] G. Manca[a],[27] A. Manousakis-Katsikakis,[3] F. Margaroli,[46] C. Marino,[24] M. Martínez,[4] R. Martínez-Ballarín,[29] P. Mastrandrea,[49] M.E. Mattson,[57] P. Mazzanti,[6] K.S. McFarland,[47] P. McIntyre,[51] R. McNulty[i],[27] A. Mehta,[27] P. Mehtala,[21] A. Menzione,[44] C. Mesropian,[48] T. Miao,[15] D. Mietlicki,[32] A. Mitra,[1] H. Miyake,[53] S. Moed,[20] N. Moggi,[6] M.N. Mondragon[k],[15] C.S. Moon,[25] R. Moore,[15] M.J. Morello,[15] J. Morlock,[24] P. Movilla Fernandez,[15] A. Mukherjee,[15] Th. Muller,[24] P. Murat,[15] M. Mussini[aa],[6] J. Nachtman[m],[15] Y. Nagai,[53] J. Naganoma,[56] I. Nakano,[38] A. Napier,[54] J. Nett,[51] C. Neu,[55] M.S. Neubauer,[22] J. Nielsen[d],[26] L. Nodulman,[2] O. Norniella,[22] E. Nurse,[28] L. Oakes,[40] S.H. Oh,[14] Y.D. Oh,[25] I. Oksuzian,[55] T. Okusawa,[39] R. Orava,[21] L. Ortolan,[4] S. Pagan Griso[bb],[41] C. Pagliarone,[52] E. Palencia[e],[9] V. Papadimitriou,[15] A.A. Paramonov,[2] J. Patrick,[15] G. Pauletta[gg],[52] M. Paulini,[10] C. Paus,[30] D.E. Pellett,[7] A. Penzo,[52] T.J. Phillips,[14] G. Piacentino,[44] E. Pianori,[43] J. Pilot,[37] K. Pitts,[22] C. Plager,[8] L. Pondrom,[58] S. Poprocki[f],[15] K. Potamianos,[46] O. Poukhov*,[13]

F. Prokoshin[y],[13] A. Pronko,[15] F. Ptohos[g],[17] E. Pueschel,[10] G. Punzi[cc],[44] J. Pursley,[58] A. Rahaman,[45]
V. Ramakrishnan,[58] N. Ranjan,[46] I. Redondo,[29] P. Renton,[40] M. Rescigno,[49] T. Riddick,[28] F. Rimondi[aa],[6]
L. Ristori[44],[15] A. Robson,[19] T. Rodrigo,[9] T. Rodriguez,[43] E. Rogers,[22] S. Rolli[h],[54] R. Roser,[15] M. Rossi,[52]
F. Rubbo,[15] F. Ruffini[dd],[44] A. Ruiz,[9] J. Russ,[10] V. Rusu,[15] A. Safonov,[51] W.K. Sakumoto,[47] Y. Sakurai,[56]
L. Santi[gg],[52] L. Sartori,[44] K. Sato,[53] V. Saveliev[u],[42] A. Savoy-Navarro,[42] P. Schlabach,[15] A. Schmidt,[24]
E.E. Schmidt,[15] M.P. Schmidt[*],[59] M. Schmitt,[36] T. Schwarz,[7] L. Scodellaro,[9] A. Scribano[dd],[44] F. Scuri,[44]
A. Sedov,[46] S. Seidel,[35] Y. Seiya,[39] A. Semenov,[13] F. Sforza[cc],[44] A. Sfyrla,[22] S.Z. Shalhout,[7] T. Shears,[27]
P.F. Shepard,[45] M. Shimojima[t],[53] S. Shiraishi,[11] M. Shochet,[11] I. Shreyber,[34] A. Simonenko,[13] P. Sinervo,[31]
A. Sissakian[*],[13] K. Sliwa,[54] J.R. Smith,[7] F.D. Snider,[15] A. Soha,[15] S. Somalwar,[50] V. Sorin,[4] P. Squillacioti,[44]
M. Stancari,[15] M. Stanitzki,[59] R. St. Denis,[19] B. Stelzer,[31] O. Stelzer-Chilton,[31] D. Stentz,[36] J. Strologas,[35]
G.L. Strycker,[32] Y. Sudo,[53] A. Sukhanov,[16] I. Suslov,[13] K. Takemasa,[53] Y. Takeuchi,[53] J. Tang,[11] M. Tecchio,[32]
P.K. Teng,[1] J. Thom[f],[15] J. Thome,[10] G.A. Thompson,[22] E. Thomson,[43] P. Ttito-Guzmán,[29] S. Tkaczyk,[15]
D. Toback,[51] S. Tokar,[12] K. Tollefson,[33] T. Tomura,[53] D. Tonelli,[15] S. Torre,[17] D. Torretta,[15] P. Totaro,[41]
M. Trovato[ee],[44] Y. Tu,[43] F. Ukegawa,[53] S. Uozumi,[25] A. Varganov,[32] F. Vázquez[k],[16] G. Velev,[15] C. Vellidis,[3]
M. Vidal,[29] I. Vila,[9] R. Vilar,[9] J. Vizán,[9] M. Vogel,[35] G. Volpi[cc],[44] P. Wagner,[43] R.L. Wagner,[15] T. Wakisaka,[39]
R. Wallny,[8] S.M. Wang,[1] A. Warburton,[31] D. Waters,[28] M. Weinberger,[51] W.C. Wester III,[15] B. Whitehouse,[54]
D. Whiteson[b],[43] A.B. Wicklund,[2] E. Wicklund,[15] S. Wilbur,[11] F. Wick,[24] H.H. Williams,[43] J.S. Wilson,[37]
P. Wilson,[15] B.L. Winer,[37] P. Wittich[f],[15] S. Wolbers,[15] H. Wolfe,[37] T. Wright,[32] X. Wu,[18] Z. Wu,[5] K. Yamamoto,[39]
J. Yamaoka,[14] T. Yang,[15] U.K. Yang[p],[11] Y.C. Yang,[25] W.-M. Yao,[26] G.P. Yeh,[15] K. Yi[m],[15] J. Yoh,[15] K. Yorita,[56]
T. Yoshida[j],[39] G.B. Yu,[14] I. Yu,[25] S.S. Yu,[15] J.C. Yun,[15] A. Zanetti,[52] Y. Zeng,[14] and S. Zucchelli[aa][6]

(CDF Collaboration[†])

[1]*Institute of Physics, Academia Sinica, Taipei, Taiwan 11529, Republic of China*
[2]*Argonne National Laboratory, Argonne, Illinois 60439, USA*
[3]*University of Athens, 157 71 Athens, Greece*
[4]*Institut de Fisica d'Altes Energies, ICREA, Universitat Autonoma de Barcelona, E-08193, Bellaterra (Barcelona), Spain*
[5]*Baylor University, Waco, Texas 76798, USA*
[6]*Istituto Nazionale di Fisica Nucleare Bologna, [aa]University of Bologna, I-40127 Bologna, Italy*
[7]*University of California, Davis, Davis, California 95616, USA*
[8]*University of California, Los Angeles, Los Angeles, California 90024, USA*
[9]*Instituto de Fisica de Cantabria, CSIC-University of Cantabria, 39005 Santander, Spain*
[10]*Carnegie Mellon University, Pittsburgh, Pennsylvania 15213, USA*
[11]*Enrico Fermi Institute, University of Chicago, Chicago, Illinois 60637, USA*
[12]*Comenius University, 842 48 Bratislava, Slovakia; Institute of Experimental Physics, 040 01 Kosice, Slovakia*
[13]*Joint Institute for Nuclear Research, RU-141980 Dubna, Russia*
[14]*Duke University, Durham, North Carolina 27708, USA*
[15]*Fermi National Accelerator Laboratory, Batavia, Illinois 60510, USA*
[16]*University of Florida, Gainesville, Florida 32611, USA*
[17]*Laboratori Nazionali di Frascati, Istituto Nazionale di Fisica Nucleare, I-00044 Frascati, Italy*
[18]*University of Geneva, CH-1211 Geneva 4, Switzerland*
[19]*Glasgow University, Glasgow G12 8QQ, United Kingdom*
[20]*Harvard University, Cambridge, Massachusetts 02138, USA*
[21]*Division of High Energy Physics, Department of Physics, University of Helsinki and Helsinki Institute of Physics, FIN-00014, Helsinki, Finland*
[22]*University of Illinois, Urbana, Illinois 61801, USA*
[23]*The Johns Hopkins University, Baltimore, Maryland 21218, USA*
[24]*Institut für Experimentelle Kernphysik, Karlsruhe Institute of Technology, D-76131 Karlsruhe, Germany*
[25]*Center for High Energy Physics: Kyungpook National University, Daegu 702-701, Korea; Seoul National University, Seoul 151-742, Korea; Sungkyunkwan University, Suwon 440-746, Korea; Korea Institute of Science and Technology Information, Daejeon 305-806, Korea; Chonnam National University, Gwangju 500-757, Korea; Chonbuk National University, Jeonju 561-756, Korea*
[26]*Ernest Orlando Lawrence Berkeley National Laboratory, Berkeley, California 94720, USA*
[27]*University of Liverpool, Liverpool L69 7ZE, United Kingdom*
[28]*University College London, London WC1E 6BT, United Kingdom*
[29]*Centro de Investigaciones Energeticas Medioambientales y Tecnologicas, E-28040 Madrid, Spain*
[30]*Massachusetts Institute of Technology, Cambridge, Massachusetts 02139, USA*

[31] Institute of Particle Physics: McGill University, Montréal, Québec, Canada H3A 2T8; Simon Fraser University, Burnaby, British Columbia, Canada V5A 1S6; University of Toronto, Toronto, Ontario, Canada M5S 1A7; and TRIUMF, Vancouver, British Columbia, Canada V6T 2A3
[32] University of Michigan, Ann Arbor, Michigan 48109, USA
[33] Michigan State University, East Lansing, Michigan 48824, USA
[34] Institution for Theoretical and Experimental Physics, ITEP, Moscow 117259, Russia
[35] University of New Mexico, Albuquerque, New Mexico 87131, USA
[36] Northwestern University, Evanston, Illinois 60208, USA
[37] The Ohio State University, Columbus, Ohio 43210, USA
[38] Okayama University, Okayama 700-8530, Japan
[39] Osaka City University, Osaka 588, Japan
[40] University of Oxford, Oxford OX1 3RH, United Kingdom
[41] Istituto Nazionale di Fisica Nucleare, Sezione di Padova-Trento, [bb] University of Padova, I-35131 Padova, Italy
[42] LPNHE, Universite Pierre et Marie Curie/IN2P3-CNRS, UMR7585, Paris, F-75252 France
[43] University of Pennsylvania, Philadelphia, Pennsylvania 19104, USA
[44] Istituto Nazionale di Fisica Nucleare Pisa, [cc] University of Pisa, [dd] University of Siena and [ee] Scuola Normale Superiore, I-56127 Pisa, Italy
[45] University of Pittsburgh, Pittsburgh, Pennsylvania 15260, USA
[46] Purdue University, West Lafayette, Indiana 47907, USA
[47] University of Rochester, Rochester, New York 14627, USA
[48] The Rockefeller University, New York, New York 10065, USA
[49] Istituto Nazionale di Fisica Nucleare, Sezione di Roma 1, [ff] Sapienza Università di Roma, I-00185 Roma, Italy
[50] Rutgers University, Piscataway, New Jersey 08855, USA
[51] Texas A&M University, College Station, Texas 77843, USA
[52] Istituto Nazionale di Fisica Nucleare Trieste/Udine, I-34100 Trieste, [gg] University of Udine, I-33100 Udine, Italy
[53] University of Tsukuba, Tsukuba, Ibaraki 305, Japan
[54] Tufts University, Medford, Massachusetts 02155, USA
[55] University of Virginia, Charlottesville, Virginia 22906, USA
[56] Waseda University, Tokyo 169, Japan
[57] Wayne State University, Detroit, Michigan 48201, USA
[58] University of Wisconsin, Madison, Wisconsin 53706, USA
[59] Yale University, New Haven, Connecticut 06520, USA

(Dated: August 4, 2011)

Diboson production ($WW + WZ + ZZ$) has been observed at the Tevatron in hadronic decay modes dominated by the WW process. This paper describes the measurement of the cross section of WZ and ZZ events in final states with large $\not\!\!E_T$ and using b-jet identification as a tool to suppress WW contributions. Due to the limited energy resolution, we cannot distinguish between partially hadronic decays of WZ and ZZ, and we measure the sum of these processes. The number of signal events is extracted using a simultaneous fit to the invariant mass distribution of the two jets for events with two b-jet candidates and events without two b-jet candidates. We measure a cross section $\sigma(p\bar{p} \to WZ, ZZ) = 5.8^{+3.6}_{-3.0}$ pb, in agreement with the standard model.

PACS numbers: 12.60.Jv, 13.85.Qk, 14.80.Ly

[*] Deceased
[†] With visitors from [a] Istituto Nazionale di Fisica Nucleare, Sezione di Cagliari, 09042 Monserrato (Cagliari), Italy, [b] University of CA Irvine, Irvine, CA 92697, USA, [c] University of CA Santa Barbara, Santa Barbara, CA 93106, USA, [d] University of CA Santa Cruz, Santa Cruz, CA 95064, USA, [e] CERN,CH-1211 Geneva, Switzerland, [f] Cornell University, Ithaca, NY 14853, USA, [g] University of Cyprus, Nicosia CY-1678, Cyprus, [h] Office of Science, U.S. Department of Energy, Washington, DC 20585, USA, [i] University College Dublin, Dublin 4, Ireland, [j] University of Fukui, Fukui City, Fukui Prefecture, Japan 910-0017, [k] Universidad Iberoamericana, Mexico D.F., Mexico, [l] Iowa State University, Ames, IA 50011, USA, [m] University of Iowa, Iowa City, IA 52242, USA, [n] Kinki University, Higashi-Osaka City, Japan 577-8502, [o] Kansas State University, Manhattan, KS 66506, USA, [p] University of Manchester, Manchester M13 9PL, United Kingdom, [q] Queen Mary, University of London, London, E1 4NS, United Kingdom, [r] University of Melbourne, Victoria 3010, Australia, [s] Muons, Inc., Batavia, IL 60510, USA, [t] Nagasaki Institute of Applied Science, Nagasaki, Japan, [u] National Research Nuclear University, Moscow, Russia, [v] University of Notre Dame, Notre Dame, IN 46556, USA, [w] Universidad de Oviedo, E-33007 Oviedo, Spain, [x] Texas Tech University, Lubbock, TX 79609, USA, [y] Universidad Tecnica Federico Santa Maria, 110v Valparaiso, Chile, [z] Yarmouk University, Irbid 211-63, Jordan, [hh] On leave from J. Stefan Institute, Ljubljana, Slovenia,

Measurements of diboson production cross sections provide tests of the self-interactions of the gauge bosons. Deviations from the standard model (SM) prediction for the production rates could indicate new physics [1, 2]. Furthermore, given that hadronic final states in diboson production are similar to associated Higgs boson production (Higgs-strahlung), $p\bar{p} \rightarrow VH + X\,(V{=}W, Z)$, the analysis techniques described in this Letter are important for Higgs boson searches [3].

Diboson production has been observed at the Tevatron in fully leptonic final states [4, 5]. In the case of partially hadronic decay modes, the CDF collaboration observed a signal for combined measurement of WW, WZ, and ZZ using an integrated luminosity of $3.5\,\mathrm{fb}^{-1}$ where the signal is dominated by WW [6, 7]. In this paper, we describe a measurement where we isolate the WZ and ZZ signals in partially hadronic decay channels by requiring the presence of b-jet candidates. We perform a fit to the dijet invariant mass spectrum (m_{jj}), splitting events into two non-overlapping classes: with at least two b-jet candidates (two-tag channel), and fewer than two b-jet candidates (no-tag channel) [24]. This ensures maximum acceptance to the $WZ+ZZ$ events, and fitting in both the two-tag and the no-tag channel improves our signal sensitivity significantly compared to using only one channel (with or without b-tagging). The signatures to which we are sensitive $WZ \rightarrow \ell\nu b\bar{b}$ and $ZZ \rightarrow \nu\nu b\bar{b}$ in the two-tag channel and all decays with unbalanced transverse momentum ($\not\!\!E_T$) in the no-tag channel ($WZ \rightarrow \ell\nu q\bar{q}, q\bar{q}'\nu\nu$ and $ZZ \rightarrow \nu\nu q\bar{q}$) [25].

We analyze a dataset of $p\bar{p}$ collisions corresponding to an integrated luminosity of $5.2\,\mathrm{fb}^{-1}$ collected with the CDF II detector at a center-of-mass energy of 1.96 TeV. The CDF II detector is described in detail elsewhere [8]. The detector is cylindrically symmetric around the proton beam axis which is oriented in the positive z direction. The polar angle, θ, is measured from the origin of the coordinate system at the center of the detector with respect to the z axis. Pseudorapidity, transverse energy, and transverse momentum are defined as $\eta{=}-\ln\tan(\theta/2)$, $E_T{=}E\sin\theta$, and $p_T{=}p\sin\theta$, respectively. The central and plug calorimeters, which respectively cover the pseudorapidity regions of $|\eta|{<}1.1$ and $1.1{<}|\eta|{<}3.6$, surround the tracking system with a projective tower geometry. The detector has a charged particle tracking system immersed in a 1.4 T magnetic field, aligned coaxially with the $p\bar{p}$ beams. A silicon microstrip detector provides tracking over the radial range 1.5 to 28 cm. A 3.1 m long open-cell drift chamber, the central outer tracker (COT), covers the radial range from 40 to 137 cm and provides up to 96 measurements with alternating axial and $\pm 2^{\circ}$ stereo superlayers. The fiducial region of the silicon detector extends to $|\eta| \sim 2$, while the COT provides coverage for $|\eta| \lesssim 1$. Muons are detected up to $|\eta| < 1.0$ by drift chambers located outside the hadronic calorimeters.

Events are selected via a set of triggers with $\not\!\!E_T$ requirements The bulk of the data is collected with a trigger threshold $\not\!\!E_T > 45$ GeV. Other triggers have a lower $\not\!\!E_T$ requirement but also include additional requirements on jets in the event, or sometimes correspond to smaller effective integrated luminosity. We measure the trigger efficiency using an independent $Z \rightarrow \mu\mu$ sample and verify that the trigger logic used does not sculpt the shape of the dijet invariant mass.

Events with large $\not\!\!E_T$ ($\not\!\!E_T > 50$ GeV) and two or more jets are selected in this analysis. Jets are reconstructed in the calorimeter using the JETCLU cone algorithm [9] with a cone radius of 0.4 in (η, ϕ) space. The energy measured by the calorimeter is corrected for effects that distort the true jet energy [10]. Such effects include the non-linear response of the calorimeter to particle energy, loss of energy in uninstrumented regions of the detector, energy radiated outside of the jet cone, and multiple proton antiproton interactions per beam crossing. The jets must have $E_T > 20$ GeV and be within $|\eta| < 2$. To suppress the multi-jet background contribution, we require the angle between the $\not\!\!E_T$ vector and any identified jet to be larger than 0.4 radians [26]. The $\not\!\!E_T$-significance, as defined in [6], measures the likelihood that the $\not\!\!E_T$ in the event comes from actual particles escaping detection as opposed to resolution effects and is typically low when $\not\!\!E_T$ arises from mis-measurements. We require $\not\!\!E_T$-significance to be larger than 4 (see [6, 11]). Beam halo events are removed by requiring the event electromagnetic fraction, defined as the ratio between the amount of energy measured in the electromagnetic calorimeter and the sum of electromagnetic and hadronic calorimeter measurements, $E_{\mathrm{EM}}/E_{\mathrm{total}}$, to be between 0.3 and 0.85. We remove cosmic ray events based on timing information from the electromagnetic and hadronic calorimeters.

To gain sensitivity to the b-quark content of our jet sample, we employ a new multivariate neural-network-based tagger that provides a figure of merit to indicate how b-like a jet appears to be. This tagger is unique in its emphasis on studying individual tracks. The tagger identifies tracks with transverse momentum $p_T > 0.4$ GeV/c which have registered hits in the innermost (silicon) tracking layers, and uses a track-by-track neural network to calculate a figure of merit for a given track's "$b$ness", *i.e.*, the likelihood that it comes from the decay of a B hadron. The observables used in the track neural network are the transverse momentum of the track in the laboratory frame, the transverse momentum of the track with respect to the jet axis, the rapidity with respect to the jet axis and the track impact parameter with respect to the primary vertex and its uncertainty.

Having the track $b$nesses, we proceed to calculate the jet-by-jet $b$nesses. The input observables used are the top five track $b$nesses in the jet cone, the number of tracks above a certain $b$ness threshold, the invariant mass of all these tracks, the uncertainty on the displaced vertex from the B hadron decay in the xy plane, and muon information for semileptonic B decays, as described in [12]. The final output of the algorithm is a number between -1 and 1, the $b$ness. By requiring values of $b$ness closer to 1, one can select increasingly pure samples of b jets. The training for the track neural network as well as the jet-by-jet network is performed using jets matched to b quarks from $Z \to b\bar{b}$ events for signal and jets not matched to b quarks for background in a PYTHIA ZZ Monte Carlo sample.

To verify that the b-tagger data response is reproduced by the Monte Carlo simulation, we use two control samples, one dominated by $Z(\to \ell\ell)$ + 1 jet events, and one dominated by $t\bar{t}$ pair events using a lepton + jets selection. The former offers a comparison of jets that largely do not originate from bottom quarks, while the latter compares jets in a heavily b-enhanced sample. We examine the $b$ness distributions in simulation and data and use these comparisons to derive a correction to the tagging efficiency and mistag rates in the Monte Carlo simulation for our jet $b$ness cuts. The mistag rate is defined as the rate of misidentification of non-b jets as b-jets.

We define our signal sample as events in the $40 < m_{jj} < 160$ GeV/c^2 region. In the calculation of the invariant mass m_{jj} we use the two jets in the events with the highest $b$ness score. The final number of events is extracted by a simultaneous fit to the dijet invariant mass distribution in the two separate channels mentioned above. Since we apply b-tagging and allow for two or more jets, $t\bar{t}$ and single t production are a significant background. To help suppress those backgrounds, we require the events to have no more than one identified lepton (electrons or muons), where a very loose lepton identification is used to increase the efficiency of this rejection. In addition, the sum of the number of identified electrons, muons and jets with $E_T > 10$ GeV must not exceed 4.

After this selection, we have four major classes of backgrounds: (1) electroweak (EWK) V boson+jet processes that are estimated using Monte Carlo simulations and cross-checked using a γ+jets data set, described below; (2) multi-jet events with generic QCD jet production which result in $\not\!\!E_T$ due to mis-measurements of the jet momenta. This background is evaluated using a data-driven method; (3) single top and top quark pair production. We estimate this background using a Monte Carlo simulation; and (4) $WW \to l\nu jj$ production. This is indistinguishable from the signal in the non-b-tagged region. This background is evaluated using a Monte Carlo simulation.

Monte Carlo simulations used for signal and background estimates are performed with a combination of PYTHIA [13], ALPGEN [14] and MADGRAPH [15] event generators interfaced with PYTHIA for parton showering. The geometric and kinematic acceptances are obtained using a GEANT-based simulation of the CDF II detector [16]. For the comparison to data, all sample cross

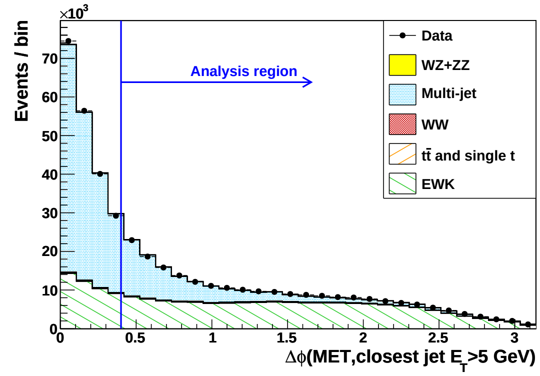

FIG. 1: Minimum azimuthal angular separation $\min(\Delta\phi(\vec{\not\!\!E}_T, \text{jet}))$ between all jets with $E_T > 5$ GeV and the missing E_T, for events that pass all of the analysis cuts except for the $\min(\Delta\phi(\vec{\not\!\!E}_T, \text{jet}))$ cut. The analysis cut is at $\min(\Delta\phi(\vec{\not\!\!E}_T, \text{jet})) > 0.4$.

sections are normalized to the results of NLO calculations performed with MCFM V5.4 program [17] and using the CTEQ6M parton distribution functions (PDFs) [18].

We use a γ+jets data sample to check our modeling of the V+jet background shape. Since the selection has a tight $\not\!\!E_T$ threshold to enhance the sensitivity to the leptonic decays of the W and Z, we emulate that selection in the γ+jets sample by vectorially adding the photon's E_T to the measured $\not\!\!E_T$. In order to account for any differences in kinematics between γ+jets and V+jets, we correct the γ+jets dijet mass shape in data based on the difference between γ+jets and V+jets Monte Carlo simulations. This way, any production difference is taken into account while effects such as detector resolution, PDF uncertainties and modeling of initial- and final-state radiation cancel. After we apply this correction to the γ+jets data, there is a residual difference between the photon data and our V+jets simulation, which we use to determine a systematic uncertainty on the shape of the V+jets background.

In the case of the multi-jet background contribution, we derive both the normalization and the shape from data. The two important cuts used to reject this background are the $\not\!\!E_T$-significance and $\min(\Delta\phi(\vec{\not\!\!E}_T, \text{jet}))$. The latter is shown in Fig. 1, which also demonstrates our ability to model the multi-jet background. To estimate the remaining multi-jet background contribution, we construct a new variable, $\not\!p_T$, to complement the traditional calorimeter-based $\not\!\!E_T$. The $\not\!p_T$ is defined as the negative vector sum of tracks with $p_T > 0.3$ GeV/c. Tracks used in the calculation of $\not\!p_T$ have to pass minimal quality requirements.

When comparing the azimuthal angle (ϕ) between $\not\!\!E_T$ and $\not\!p_T$, we expect the two quantities to align in the case of true $\not\!\!E_T$ (*e.g.*, for diboson signal and electroweak backgrounds). The difference between these two angles is referred to as $\Delta\phi_{MET}$. Electroweak backgrounds (and diboson signal) will be present in all regions, but will dominate at low $\Delta\phi_{MET}$ due to correctly measured $\not\!\!E_T$ from neutrinos. To determine the dijet mass shape of the multi-jet background, we subtract all other background predictions obtained with Monte Carlo simulations from data, in the multi-jet enhanced region with $\Delta\phi_{MET} > 1$. The normalization of the template obtained this way is then corrected to account for those events with $\Delta\phi_{MET} \leq 1$ using a multi-jet Monte Carlo sample; this correction introduces a 7% uncertainty on the normalization of the multi-jet background. The uncertainty on the shape of the distribution is estimated comparing the difference in dijet mass shapes for $\Delta\phi_{MET} > 1$ and $\Delta\phi_{MET} < 1$ in a control sample defined by $3 < \not\!\!E_T$-significance < 4.

We extract the number of signal events with a binned maximum likelihood fit to data using the method described in [19]. We supply template histograms for backgrounds and signals and perform a simultaneous fit in two channels, defined by different $b$ness thresholds. The templates, and the uncertainties on their normalizations, are listed below. (1) EWK background (W/Z+jets): Normalizations are allowed to float in the fit, unconstrained, with no correlation between the two channels. (2) $t\bar{t}$ and single top: The uncertainties on the theoretical cross sections of these processes are 6% [20] and 11% [21, 22], respectively. We treat these uncertainties as completely correlated, which translates to an uncertainty of 5.8% on the normalization of the no-tag channel template, and 5.4% on the normalization of the two-tag channel template, due to the relative contributions of each process. (3) Multi-jet background: We use our data-driven estimate, Gaussian constrained with an uncertainty of 7% in the no-tag channel. Because there are very few events in the two-tag channel template, we assign a normalization uncertainty equal to the statistical uncertainty ($\sqrt{N}/N$, 11%) of the template. The uncertainties in the two channels are treated as uncorrelated. (4) WW: We use the NLO cross section and apply a Gaussian constraint to the number of WW events centered on this value with a width equal to the theoretical uncertainty of 6% [17]. (5) WZ/ZZ signal: As this is our signal, its normalization is allowed to float unconstrained in the fit. We assume that each signal process contributes proportionally to its predicted SM cross section: 3.6 pb for WZ and 1.5 pb for ZZ ([17]) corrected for our selection's acceptance and efficiencies.

In addition to uncertainties on the normalizations of each template, we consider other systematic uncertainties that may affect the shape of templates. Shape uncertainties have been described for the electroweak and multi-jet backgrounds previously. For top and diboson samples, we consider the impact of the jet energy scale (2% and 7%, respectively) and the effect that uncertainties due to the differences between jet $b$ness behavior in data and Monte Carlo simulation may have on the templates' shapes and normalizations (14% for tags and 25% for mistags, for the latter). All of the above uncertainties are treated as nuisance parameters and are incorporated into the fit using a Bayesian marginalization technique [19].

We choose the jet $b$ness thresholds that define our two fitting channels to optimize the significance of our final result. The optimization for the two-tag channel points to a broad region where the sensitivity is maximized and we choose our $b$ness thresholds in that region. The optimization favors that all remaining events be combined in a no-tag channel, rather than a single-tag channel with a low $b$ness threshold.

Process	Fit N_{events} (no-tag)	Fit N_{events} (two-tag)
EWK	$149900\,^{+5600}_{-5200}$	749 ± 48
$t\bar{t}$ and single t	$900\,^{+59}_{-61}$	$217\,^{+23}_{-27}$
Multi-jet	$76600\,^{+4900}_{-5300}$	76 ± 9.0
WW	2700 ± 200	$10\,^{+2.1}_{-2.3}$
WZ/ZZ	$1330\,^{+710}_{-690}$	$52\,^{+24}_{-23}$

TABLE I: Extracted number of events from the 2-channel fit for WZ/ZZ, with all systematics applied.

Figure 2 shows the results of the fit, and Table I shows the number of fitted events.

To translate the result of our fit to the data to bounds or limits on the cross section of WZ/ZZ production, we construct Feldman-Cousins bands by analyzing the distribution of fitted (*i.e.*, measured) cross sections in pseudo experiments generated with a variety of scale factors on the input signal cross section [23]. When running pseudo experiments, we consider the effect of additional systematic uncertainties that affect our acceptance. These include, in order of increasing significance: jet energy resolution (0.7%), $\not\!\!E_T$ modeling (1.0%), initial and final state radiation (2.5%), parton distribution function (2.0%), and luminosity and trigger efficiency uncertainties (6.4%).

Based on a Monte Carlo simulation, the acceptance times efficiency for the WZ and ZZ production is 4.1%, and 4.6%, respectively. Our measured result, using the 1σ bands from the Feldman-Cousins analysis, is $\sigma(p\bar{p} \rightarrow WZ, ZZ) = 5.8^{+3.6}_{-3.0}$ pb, in agreement with the standard model prediction $\sigma_{SM} = 5.1$ pb ([17]). We set a limit on $\sigma_{WZ,ZZ} < 13$ pb ($2.6 \times \sigma_{SM}$) with 95% C.L. The techniques used here, in particular the b tagging algorithm, are being integrated in the current generation of searches for a low-mass Higgs boson.

We thank the Fermilab staff and the technical staffs of the participating institutions for their vital contributions. This work was supported by the U.S. Department of Energy and National Science Foundation; the Italian Istituto Nazionale di Fisica Nucleare; the Ministry of Education, Culture, Sports, Science and Tech-

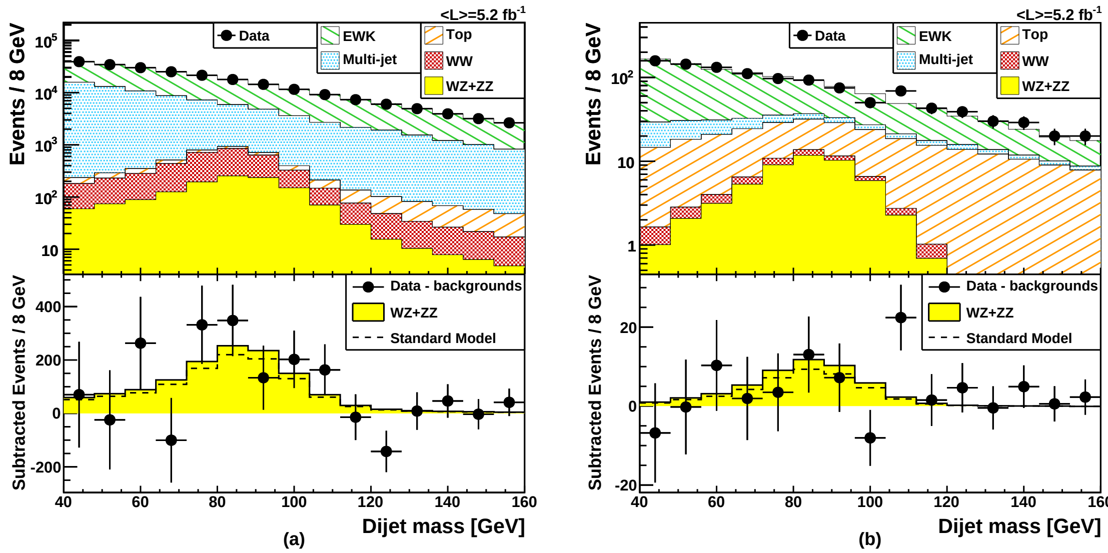

FIG. 2: Result of the fit to data for the double fit to all of WZ/ZZ. Left column is the no-tag channel; right column is the two-tag channel. Bottom row shows data after the background subtraction.

nology of Japan; the Natural Sciences and Engineering Research Council of Canada; the National Science Council of the Republic of China; the Swiss National Science Foundation; the A.P. Sloan Foundation; the Bundesministerium für Bildung und Forschung, Germany; the Korean World Class University Program, the National Research Foundation of Korea; the Science and Technology Facilities Council and the Royal Society, UK; the Institut National de Physique Nucleaire et Physique des Particules/CNRS; the Russian Foundation for Basic Research; the Ministerio de Ciencia e Innovación, and Programa Consolider-Ingenio 2010, Spain; the Slovak R&D Agency; the Academy of Finland; and the Australian Research Council (ARC).

[1] K. Hagiwara et al., Nucl. Phys. **B 282**, 253 (1987).
[2] B. Kober, B. Koch, and M. Bleicher, Phys. Rev. D **76**, 125001 (2007).
[3] T. Aaltonen et al. (CDF Collaboration), Phys. Rev. Lett. **104**, 141801 (2010).
[4] T. Aaltonen et al. (CDF Collaboration), Phys. Rev. Lett. **104**, 201801 (2010).
[5] V. M. Abazov et al. (D0 Collaboration), Phys. Rev. Lett. **103**, 191801 (2009).
[6] T. Aaltonen et al. (CDF Collaboration), Phys. Rev. Lett. **103**, 091803 (2009).
[7] T. Aaltonen et al. (CDF Collaboration), Phys. Rev. Lett. **104**, 101801 (2010).
[8] A. Abulencia et al. (CDF Collaboration), J. Phys. G **34**, 2457 (2007).
[9] F. Abe et al. (CDF Collaboration), Phys. Rev. D **45**, 1448 (1992).
[10] A. Bhatti et al., Nucl. Instrum. Methods A **566**, 375 (2006).
[11] M. Goncharov et al., Nucl. Instrum. Methods A **565**, 543 (2006).
[12] T. Aaltonen et al. (CDF Collaboration), Phys. Rev. D **79**, 052007 (2009).
[13] T. Sjöstrand et al., J. High Energy Phys. **05**, 026 (2006).
[14] M. L. Mangano et al., J. High Energy Phys. **07**, 001 (2003).
[15] J. Alwall et al., J. High Energy Phys. **09**, 028 (2007).
[16] R. Brun et al. (1978), CERN Report CERN-DD-78-2-REV (unpublished).
[17] J. M. Campbell and R. K. Ellis, Phys. Rev. D **60**, 113006 (1999).
[18] J. Pumplin et al., J. High Energy Phys. **0207**, 012 (2002).
[19] T. Aaltonen et al. (CDF Collaboration), Phys. Rev. D **82**, 112005 (2010).
[20] U. Langenfeld, S. Moch, and P. Uwer, Phys. Rev. D **80**, 054009 (2009).
[21] N. Kidonakis, Phys. Rev. D **74**, 114012 (2006).
[22] N. Kidonakis, PoS(DIS2010) **196** (2010), arXiv:1005.3330v1.
[23] G. J. Feldman and R. D. Cousins, Phys. Rev. D **57**, 3873 (1998).
[24] This last sample also contains WW events
[25] We define the missing transverse momentum $\vec{\not\!\!E}_T \equiv -\sum_i E_{\mathrm{T}}^i \mathbf{n}_i$, where $\mathbf{n}_i$ is the unit vector in the azimuthal plane that points from the beamline to the ith calorimeter tower. We call the magnitude of this vector $\not\!\!E_T$
[26] All jets in the region $|\eta| < 3.6$ and $E_T > 5$ GeV are considered